Simultaneous detection and quantification of adenine nucleotides in mammalian cultured cells by HPLC

Beatriz Kopel, Fernanda Manso Prado, Sofia Lígia Guimarães Ramos, Rafael Dias de Moura, Paolo Di Mascio, Nícolas Carlos Hoch, Marisa Helena Gennari de Medeiros, Nadja Cristhina de Souza Pinto*

Dept. de Bioquímica, Instituto de Química, Universidade de São Paulo, SP 05508-000, Brazil.

* To whom correspondence should be addressed: nadja@iq.usp.br

Keywords: adenine nucleotide quantification, RP-HPLC, ATP/ADP ratio, NAD+/NADH ratio

Abstract

Adenine nucleotides, such as ATP, ADP, ADP-ribose, AMP, NAD^+ and NADH, have central roles in cellular homeostasis and participate in several pathways. Because of their diverse roles in cell biology, accurately quantifying these metabolites is paramount for several research areas such as bioenergetics, signaling, cancer and others. There are several methods available to analyze adenine nucleotides, ranging from enzymatic assays to mass spectrometry approaches, however, to our knowledge, no method in the literature quantifies these six adenine nucleotides simultaneously, mostly due to limitations in sample preparation or detection methods. Here, we developed a method that can detect simultaneously ATP, ADP, ADP-ribose, AMP, NAD^+ and NADH using RP-HPLC with UV-Vis detection. This methodological approach is simple, sensitive to physiological concentrations of all nucleotides and detects biologically significant variations in ATP, AMP and NAD^+ induced by pharmacological treatments, presenting an accessible and accurate alternative for quantification of these nucleotides in biological samples.

Introduction

Adenine nucleotides have essential roles in biological systems, from energy metabolism to signaling. Adenosine triphosphate (ATP), through coupled reactions, is the major driver of thermodynamically unfavorable reactions in biological systems, being dubbed as the “energy currency” for cellular processes [1,2]. ATP is also the main phosphate donor for phosphorylation reactions catalyzed by kinases regulating many signaling pathways, while ATP and adenosine diphosphate (ADP) can also act as signaling molecules themselves in pathways such as purinergic signaling and others

[3]. Adenosine monophosphate (AMP), the hydrolysis product of ADP, can be generated in high energy demand situations and act as a central regulator in energy sensing pathways, such as the AMP-activated protein kinase (AMPK) pathway [4]. AMPK regulates several other downstream pathways such as glucose and lipid metabolism, cell growth, autophagy, and other pathways, reviewed in [5].

Oxidized nicotinamide dinucleotide (NAD^+) plays a pivotal role in redox reactions in the cell, acting as a coenzyme in important processes such as glycolysis, fatty acid oxidation, the citric acid cycle and others [6,7]. The ratio of NAD^+ to its reduced form, NADH, is an indicator of the cell's reducing potential and an important regulator of several cellular responses. NAD(P)H is one of the main sources of reducing power for antioxidant systems, such as the glutathione peroxidase cycle, which depends on $NADP^+$, produced by phosphorylation of NAD^+ [8], to reoxidize the enzyme [9].

In addition to their canonical bioenergetic roles, adenine nucleotides also have important roles in genomic stability. In response to DNA damage, poly-ADP-ribose polymerase 1 (PARP1) uses NAD^+ as a substrate to catalyze the formation of poly-ADP-ribose (PAR) chains, in which the ADP-ribose (ADPr) moiety of NAD^+ is covalently attached to target proteins, with concomitant release of nicotinamide [10]. PARP1 catalytic activity is induced by DNA damage, particularly single-strand breaks, and modifies histones surrounding the breaks site with PAR chains, facilitating the recruitment of the DNA repair machinery [11,12]. Upon resolution of the lesion, PAR chains are removed by hydrolases such as poly-ADP-ribose glycohydrolase (PARG) generating free ADPr monomers, which can be recycled back into NAD^+ by the NAD salvage pathway [13,14].

Considering their widespread and pivotal roles in biology, quantification of ATP, ADP and AMP in biological samples is performed since the early 1950s, mostly by enzymatic and chromatographic methods. Initially, ATP, ADP and AMP were analyzed by ion-exchange chromatography with a borate complex, although only after several sample processing steps to separate the nucleotides before the chromatographic run [15,16]. In 1954, the first protocol using luminescence to determine ATP concentration was established, only five years after the discovery that ATP could stimulate light emission in firefly lantern extracts [17]. This protocol was later adapted to use purified luciferin/luciferase and, by using a series of enzymatic treatments to convert ADP and AMP to ATP, was used to determine concentrations of ATP, ADP and AMP in biological samples, providing the basis for most luciferase-based ATP quantification kits available on the market [18].

Analytical methods, such as reverse phase high performance liquid chromatography (RP-HPLC) and liquid chromatography tandem mass spectrometry (LC-MS/MS) have also been developed to quantify these three adenine nucleotides simultaneously in biological samples [19]. However, while LC-MS/MS allows for lower limits of quantification (LOQ), its use has been limited by the difficulty in separating the three nucleotides using chromatography mobile phases compatible with MS, and by

the fact that often ATP and ADP degrade into AMP in the ionization source, compromising the precise quantification of the latter [20].

The simultaneous quantification of NAD^+ and NADH has also been challenging, as these metabolites have different optimal pHs for stability; while NAD^+ is more stable in acidic pH, NADH is stabilized under alkaline pH, likely due to the proton-catalyzed autoxidation of this species [21], with the need for quick quenching of the metabolite during the sample preparation step [22]. Nonetheless, NAD^+ and NADH have been successfully determined by colorimetric assays [23], fluorescence spectrophotometry [24], and by LC-MS/MS methods, as reviewed in [21].

Methods for measuring free ADPr are limited, as studies have so far mostly focused on its polymerized form, PAR. In biological samples, the most commonly used tools to measure PAR are antibody-based [25]. Measurements of free ADPr are rather scarce, being done in *in vitro* studies that measure PARP1 activity by HPLC [26], or together with NAD^+ using acidic extraction conditions from yeast [27] and mammalian cells [20], both using LC-MS/MS.

However, to our knowledge, so far, no analytical method has been developed to quantify these six metabolically relevant adenine nucleotides (ATP, ADP, AMP, ADPr, NAD^+ and NADH, Figure 1) simultaneously. To address this, we developed a method to detect them using RP-HPLC with UV-Vis detection, in the same biological sample. This approach diminishes the number of experimental replicas required to measure all nucleotides and cuts sample preparation and analysis time significantly, therefore making it more sustainable and user-friendly. Moreover, HPLC is a cheaper and more accessible alternative to LC-MS/MS. Nonetheless, the HPLC method developed here has limits of detection compatible with physiological ranges of all six metabolites in cultured human cells. Moreover, validation experiments with pharmacological agents that are known to alter concentrations of ATP, AMP and NAD+ confirmed that this method detects biologically relevant variations in these nucleotides.

Materials and methods

1. Cell culture and treatments

MRC-5 normal human pulmonary fibroblasts were maintained in DMEM high glucose containing 10% fetal bovine serum + 1% penicillin/streptomycin (complete medium) at 37 °C under 5% CO_2 atmosphere. Cultures were routinely subcultured using 0.5% trypsin when 80% confluence was reached. For the treatments, cells were seeded in 100 mm plates and incubated with 20 µM carbonyl cyanide p-trifluoromethoxy phenylhydrazone (FCCP) for 1 h; 20 mM 2-deoxyglucose (2-deoxyGlu) + 1 µM oligomycin for 2:30 h; or 10 nM FK866 for 24 h. All treatments were carried out in complete medium, while control cells received 0.01% DMSO, as vehicle control.

2. Nucleotide extraction

Figure 2 depicts the experimental workflow for extraction and analysis of samples. Cells grown on 100 mm dishes were treated as described above and carefully washed with phosphate-buffer saline (PBS). After PBS removal, 1 mL of HPLC-grade methanol (Merck) containing 1 mM deferoxamine mesylate (Sigma-Aldrich) was added to the plate and the contents homogenized with a cell scraper. The cell extracts were then transferred to a 2 mL microtube and incubated for two hours at 25 ºC with a 1,300-rpm agitation in a Thermomixer C (Eppendorf). Subsequently, samples were centrifuged at 20,000g for 10 minutes at 4 ºC. The supernatant, which contains all nucleotides, was stored at -80 ºC. The samples were dried at 20 ºC in a SpeedVac and then stored again at – 80ºC until the analysis. The pellet was stored at – 20 ºC for protein quantification.

3. Protein purification and quantification

The pellets obtained after nucleotide extraction were suspended in 250 µL of freshly prepared extraction buffer (100 mM ammonium bicarbonate, 8 M urea) and mixed in a Thermomixer at 25 ºC until completely dissolved. When pellet solubilization was not complete, samples were mixed at 1,000 rpm at 55 ºC in a Thermomixer for as long as needed. Subsequently, 1 mL of ice-cold acetone was added to the samples and vortexed thoroughly. Samples were kept at – 20 ºC overnight for protein precipitation followed by centrifugation at 13,000g for 10 minutes at 4 ºC. The supernatant was completely removed, and samples were air-dried in a fume hood. The dry pellets were resuspended in 200 µL of extraction buffer and used for protein quantification. Before quantification, samples were diluted so the final concentration of urea did not exceed 3 M, to avoid interferences in the protein quantification methods. We used Bio-Rad Protein Assay Dye Reagent Concentrate (Bio-Rad) according to the manufacturer's instruction, and bovine gamma globulin (Bio-Rad) as standard.

4. RP-HPLC analysis

All analytes were analyzed in a single run using a Luna C18/2 5 µm 100 Å 250 x 4.6 mm column (Phenomenex). Two mobile phases were utilized: phase A being 25 mM diammonium hydrogen phosphate ($(NH_4)_2HPO_4$) at pH 6,0, adjusted using 85% phosphoric acid, and phase B being HPLC-grade methanol. Column oven temperature was 25ºC and the flow was 0,8 mL/min. Samples were separated using the following gradient: 0-10 min 1% B, 10-15 min 1%-20% B, 15-20 min 20% B, 20-22 min 20%-40% B, 22-27 min 40% B, 27-30 min 40%-1% B, 30-40 min 1% B. Analytes were monitored at 254 nm.

Dried samples prepared as above were resuspended in 100 µL of phase A, agitated at 1,000 rpm for 10 min at 37 ºC, and centrifuged at room temperature for 10 min at 10,000g. The supernatant was transferred to a new tube and 45 µL were injected per analysis. The same injection volume was also used to prepare the standard curves, which consisted of solutions in the 0.1 to 200 µg/mL concentration range for each analyte.

We note that to ensure the reliability of the standard curves, all standards must be freshly prepared immediately before the experiment, as we observed that ATP and NADH are rapidly degraded when stored at -20 ºC (not shown).

5. Recovery assay for estimation of analyte loss during the experimental procedure

To estimate the loss of each metabolite during the nucleotide extraction process, samples containing all analytical standards were submitted to similar processing as the biological samples and the peak areas obtained in RP-HPLC analysis were then compared to the area of control samples, which were not submitted to extraction. For this test, ATP, ADP, ADP-ribose and AMP were tested together to account for the possibility of nucleotide hydrolysis into AMP during the extraction process. NAD^+ and NADH were evaluated separately. Loss rates were calculated as the percentage of peak area lost after extraction and used as correction factors in the calculation of the concentration for biological samples.

6. Statistical analysis

Linear regressions were obtained using GraphPad Prism 10 or Origin 2024. To evaluate statistical significance, one-way ANOVA with a Tukey post-hoc test for each metabolite using GraphPad Prism 10.

Results and discussion

1. Sample preparation procedure

Several methods have been published to prepare samples for adenine nucleotide quantification using different approaches. A key common point between different methods is metabolic quenching, fundamental to maintaining nucleotide concentrations as close as possible to intact cellular levels. One common method of metabolic quenching is acidification, inactivating ATPases to preserve the ATP concentration [28,29]. This is incompatible with experimental designs that require the

simultaneous analysis of NAD^+ and NADH, as NADH is spontaneously converted to NAD^+ in acidic conditions [21], altering the relative concentration of these metabolites.

To circumvent this problem, metabolic quenching can also be achieved by the use of organic solvents, such as methanol or combinations of solvents, [30,31], which is the method we chose here. To preserve the cellular NAD^+/NADH ratio during the isolation, we used 100 mM deferoxamine mesylate, an iron chelating agent, in 100% methanol, as we found this combination to effectively reduce metabolite loss in the sample preparation steps (data not shown).

2. RP-HPLC provides a complete separation of six metabolites and low LOQ

Many relevant biological processes result in variations in absolute concentration or in the ratio between adenine nucleotides, so that it is relevant to be able to quantify all these species, preferably in the same samples to avoid artifacts due to sample manipulation. Thus, we sought to develop an HPLC protocol that would allow for simultaneous determination of six adenine nucleotides highly relevant in the context of energy metabolism in mammalian cells: ATP, ADP, AMP, NAD+, NADH and ADP-ribose. As shown in Figure 3, the chromatography conditions established here yielded a good separation of all six analytes, with distinct peaks for each, which did not overlap. It is important to point out that the standard runs, like the one shown in Figure 3A, used solutions containing all nucleotides, except NADH. NADH standard runs were performed separately to avoid compromising quantification of NAD^+, due to artifactual oxidation of NADH. Even in the standard run, a small peak at the NAD^+ retention time in the NADH standard curve was detected (arrow), illustrating this problem (red line). Figure 3 shows the individual standard curves for all 6 nucleotides.

Using standards, we determined both the loss rate for each analyte due to experimental manipulation, and the minimal concentration to be experimentally quantified for each analyte, referred to as limit of quantification (LOQ). For ATP, ADP, ADPr and NAD^+, loss rates were quite similar, with an average of 16.82% loss (Table 1). This is quite relevant when dealing with biological samples, as extensive loss due to experimental manipulation could hinder quantification, if the concentrations obtained after all procedures would fall below the LOQ. Altogether, the low LOQ and low loss rate for these nucleotides make this method very useful and sensitive for biological samples.

On the other hand, AMP and NADH show distinct loss rates from the other nucleotides analyzed here (Table 1). In the ATP, ADP, ADPr and AMP mix, we observed more AMP being detected after the extraction process, hence the negative loss rate for AMP. It is likely that AMP concentration was increased due to spontaneous hydrolysis of ATP and ADP into AMP during the procedure. NADH, presented a higher loss rate than other metabolites, at 30.27%, which could be partially explained by oxidation to NAD^+. These results highlight the importance of the

loss rate analysis for each individual analyte and in each type of experimental procedure, and of not generalizing loss rates as intrinsic of the extraction method, but more as a variable that depends on the nature and reactivity of the molecules being manipulated.

The LOQ is also a central parameter for methods developed for biological samples, as the biological concentrations of analytes may fall close to or below safe limits of detection. The values obtained using the improved HPLC method described here, presented in Table 1, range from 150 to 288 nM, compatible with the analysis of biological samples, in which most of the metabolites are present in the mM range [32].

3. Validation experiments with human cultured cells show reproducibility of expected biological responses

To validate the present method to quantify biologically relevant variations in adenine nucleotide concentrations, MRC-5 cells were treated with conditions known to modulate levels of the analytes of interest. The first treatment was with the nicotinamide phosphoribosyl transferase (NAMPT) inhibitor FK866 [33], to induce a reduction in the NAD^+ levels due to the impairment of the NAD^+ synthesis salvage pathway. The second treatment was with the oxidative phosphorylation uncoupler FCCP, which increases mitochondrial respiration that would result in decreased NADH levels. Lastly, the third treatment was a combination of oligomycin, an inhibitor of the ATP synthase, and 2-deoxyglucose, a strong inhibitor of the glycolytic pathway, which in combination should result in a decrease in ATP and an increase in AMP levels. The samples were processed as described, and typical chromatograms of the treated samples are presented in Figure 4A. Visual comparison of peak heights in the different samples clearly shows that the treatments induced visible alterations in the concentrations of the metabolites. The peak areas were, then, integrated, and the quantitative results are shown in Figures 4B-G.

As expected, FK866 treatment induced a significant decrease in the NAD^+ concentration (Figure 4F) (p-value < 0,05 relative to both controls), with a slight decrease in NADH (Figure 4G), which was not statistically significant. However, the NAD^+/NADH ratio did not changed significantly after FK866 treatment (Figure 4J), because of the simultaneous decrease in both NAD^+ and NADH, highlighting the importance of measuring individual concentration of these nucleotides, as opposed to ratios.

The results obtained after the combined treatment of oligomycin and 2-deoxyglucose (O2D) also support the notion that ratios may not reflect biologically relevant changes. While statistically significant differences in ATP (Figure 4B) and AMP (Figure 4E) concentrations were observed, ATP/ADP and ATP/AMP ratios were not statistically different in treated and control samples. For the ATP/AM ratio, it is

likely that the relatively large sample variation contributed to the lack of statistical significance.

Conclusion

Given the relevance of adenine nucleotides in biological processes, it is paramount to have analytical methods to adequately quantify these nucleotides in biological samples. However, the use of several analytical methods is limited by the high salt concentrations used in the sample preparation steps for these methods. In addition, some of the instrumentation needed in these assays, like mass spectrometry, may not be readily available to most cell biology labs. With that in mind, we developed an improved method that uses HPLC-DAD detection to analyze six adenine nucleotides in a single run. The method uses a simple and fast sample preparation procedure that allows for dry sample storage, so that the biological experiments can be performed independently and the HPLC analyses can be run in parallel, increasing reproducibility. In addition, the organic extraction and the use of desferoxamine minimizes artifactual degradation of analytes, improving accurate quantification. Moreover, the simultaneous determination of all six adenine nucleotides may also contribute to decreased inter sample variation and increased accuracy.

We also showed that this method is sensitive enough to detect biologically relevant variations in mammalian cells in culture, with average cellular concentrations well within the limit of detection for each analyte. More importantly, our results using known pharmacological bioenergetic interventions highlight the importance of measuring absolute concentrations of the nucleotides, rather than ratios, as the latter may not reflect biologically relevant effects.

Considering the easily adaptable sample preparation and separation procedures and the sensitivity of this method, we propose that it could be used as a more accessible alternative to LC-MS/MS analysis for adenine nucleotides in biological samples of varying natures.

Acknowledgements

This work was supported by Fundação de Amparo à Pesquisa do Estado de São Paulo (FAPESP) grants 2024/07910-7 to NCS-P, CEPID Redoxoma 2013/07937–8 to PDM and MHGM, and 2018/18007-5 to NCH. BK is the recipient of FAPESP fellowship 2022/16432-6, RDM is the recipient of FAPESP fellowship 2020/02701-0, and SLRG is supported by Coordenação de Aperfeiçoamento de Pessoal de Nível Superior (CAPES). MHGM and PDM are supported by Universidade de São Paulo (USP) NAP Redoxoma (PRPUSP 2011.1.9352.1.8). NCS-P is supported by Conselho Nacional de Desenvolvimento Científico e Tecnológico (CNPq) grant 311588/2021-2, MHGM is supported by CNPq grant 304945/2021-8, and PDM is supported by CNPq grant

304350/2023-0 and John Simon Guggenheim Memorial Foundation. We thank Adriana M. P. Wendel for technical assistance.

Author contributions

BK, conceptualization, investigation, writing-original draft; FMP, investigation; RDM, investigation; SLGR, investigation; PDM, funding acquisition, writing-review and editing; NCH, funding acquisition, writing-review and editing; MHGM, funding acquisition, writing-review and editing; NCS-P, conceptualization, funding acquisition, supervision, writing-original draft.

References

(1) Nelson, D. L.; Cox, M. M.; Hoskins, A. A.; Lehninger, A. L. *Lehninger Principles of Biochemistry*, Eighth edition.; Macmillan International Higher Education: New York, 2021.
(2) Knowles, J. R. Enzyme-Catalyzed Phosphoryl Transfer Reactions. *Annu. Rev. Biochem.* **1980**, *49* (1), 877–919. https://doi.org/10.1146/annurev.bi.49.070180.004305.
(3) Huang, Z.; Xie, N.; Illes, P.; Di Virgilio, F.; Ulrich, H.; Semyanov, A.; Verkhratsky, A.; Sperlagh, B.; Yu, S.-G.; Huang, C.; Tang, Y. From Purines to Purinergic Signalling: Molecular Functions and Human Diseases. *Sig Transduct Target Ther* **2021**, *6* (1), 162. https://doi.org/10.1038/s41392-021-00553-z.
(4) Hardie, D. G. AMP-Activated Protein Kinase—an Energy Sensor That Regulates All Aspects of Cell Function. *Genes Dev.* **2011**, *25* (18), 1895–1908. https://doi.org/10.1101/gad.17420111.
(5) Mihaylova, M. M.; Shaw, R. J. The AMPK Signalling Pathway Coordinates Cell Growth, Autophagy and Metabolism. *Nat Cell Biol* **2011**, *13* (9), 1016–1023. https://doi.org/10.1038/ncb2329.
(6) Amjad, S.; Nisar, S.; Bhat, A. A.; Shah, A. R.; Frenneaux, M. P.; Fakhro, K.; Haris, M.; Reddy, R.; Patay, Z.; Baur, J.; Bagga, P. Role of NAD+ in Regulating Cellular and Metabolic Signaling Pathways. *Molecular Metabolism* **2021**, *49*, 101195. https://doi.org/10.1016/j.molmet.2021.101195.
(7) Cantó, C.; Menzies, K. J.; Auwerx, J. NAD+ Metabolism and the Control of Energy Homeostasis: A Balancing Act between Mitochondria and the Nucleus. *Cell Metabolism* **2015**, *22* (1), 31–53. https://doi.org/10.1016/j.cmet.2015.05.023.
(8) Ying, W. NAD+ and NADH in Cellular Functions and Cell Death. *Front Biosci* **2006**, *11* (1), 3129. https://doi.org/10.2741/2038.
(9) Pei, J.; Pan, X.; Wei, G.; Hua, Y. Research Progress of Glutathione Peroxidase Family (GPX) in Redoxidation. *Front. Pharmacol.* **2023**, *14*, 1147414. https://doi.org/10.3389/fphar.2023.1147414.
(10) Lüscher, B.; Ahel, I.; Altmeyer, M.; Ashworth, A.; Bai, P.; Chang, P.; Cohen, M.; Corda, D.; Dantzer, F.; Daugherty, M. D.; Dawson, T. M.; Dawson, V. L.; Deindl, S.; Fehr, A. R.; Feijs, K. L. H.; Filippov, D. V.; Gagné, J.; Grimaldi, G.; Guettler, S.; Hoch, N. C.; Hottiger, M. O.; Korn, P.; Kraus, W. L.; Ladurner, A.; Lehtiö, L.; Leung, A. K. L.;

Lord, C. J.; Mangerich, A.; Matic, I.; Matthews, J.; Moldovan, G.; Moss, J.; Natoli, G.; Nielsen, M. L.; Niepel, M.; Nolte, F.; Pascal, J.; Paschal, B. M.; Pawłowski, K.; Poirier, G. G.; Smith, S.; Timinszky, G.; Wang, Z.; Yélamos, J.; Yu, X.; Zaja, R.; Ziegler, M. ADP-ribosyltransferases, an Update on Function and Nomenclature. *The FEBS Journal* **2022**, *289* (23), 7399–7410. https://doi.org/10.1111/febs.16142.

(11) Caldecott, K. W. DNA Single-Strand Break Repair and Human Genetic Disease. *Trends in Cell Biology* **2022**, *32* (9), 733–745. https://doi.org/10.1016/j.tcb.2022.04.010.

(12) Ying, S.; Chen, Z.; Medhurst, A. L.; Neal, J. A.; Bao, Z.; Mortusewicz, O.; McGouran, J.; Song, X.; Shen, H.; Hamdy, F. C.; Kessler, B. M.; Meek, K.; Helleday, T. DNA-PKcs and PARP1 Bind to Unresected Stalled DNA Replication Forks Where They Recruit XRCC1 to Mediate Repair. *Cancer Research* **2016**, *76* (5), 1078–1088. https://doi.org/10.1158/0008-5472.CAN-15-0608.

(13) Barkauskaite, E.; Jankevicius, G.; Ladurner, A. G.; Ahel, I.; Timinszky, G. The Recognition and Removal of Cellular Poly(ADP -ribose) Signals. *The FEBS Journal* **2013**, *280* (15), 3491–3507. https://doi.org/10.1111/febs.12358.

(14) Moura, R. D. D.; Mattos, P. D. D.; Valente, P. F.; Hoch, N. C. Molecular Mechanisms of Cell Death by Parthanatos: More Questions than Answers. *Genet. Mol. Biol.* **2024**, *47* (suppl 1), e20230357. https://doi.org/10.1590/1678-4685-gmb-2023-0357.

(15) Strehler, B.; Totter, J. Determination of ATP and Related Compounds. *Methods of biochemical analysis* **1954**, *1*, 341–355.

(16) Khym, J. X.; Cohn, W. E. The Separation of Sugar Phosphates by Ion Exchange with the Use of the Borate Complex[1]. *J. Am. Chem. Soc.* **1953**, *75* (5), 1153–1156. https://doi.org/10.1021/ja01101a043.

(17) McElroy, W. D. The Energy Source for Bioluminescence in an Isolated System. *Proc. Natl. Acad. Sci. U.S.A.* **1947**, *33* (11), 342–345. https://doi.org/10.1073/pnas.33.11.342.

(18) Kimmich, G. A.; Randles, J.; Brand, J. S. Assay of Picomole Amounts of ATP, ADP, and AMP Using the Luciferase Enzyme System. *Analytical Biochemistry* **1975**, *69* (1), 187–206. https://doi.org/10.1016/0003-2697(75)90580-1.

(19) Menegollo, M.; Tessari, I.; Bubacco, L.; Szabadkai, G. Determination of ATP, ADP, and AMP Levels by Reversed-Phase High-Performance Liquid Chromatography in Cultured Cells. *Methods Mol Biol* **2019**, *1925*, 223–232. https://doi.org/10.1007/978-1-4939-9018-4_19.

(20) Trammell, S. A.; Brenner, C. TARGETED, LCMS-BASED METABOLOMICS FOR QUANTITATIVE MEASUREMENT OF NAD + METABOLITES. *Computational and Structural Biotechnology Journal* **2013**, *4* (5), e201301012. https://doi.org/10.5936/csbj.201301012.

(21) Braidy, N.; Villalva, M. D.; Grant, R. NADomics: Measuring NAD+ and Related Metabolites Using Liquid Chromatography Mass Spectrometry. *Life* **2021**, *11* (6), 512. https://doi.org/10.3390/life11060512.

(22) Airhart, S. E.; Shireman, L. M.; Risler, L. J.; Anderson, G. D.; Nagana Gowda, G. A.; Raftery, D.; Tian, R.; Shen, D. D.; O'Brien, K. D. An Open-Label, Non-Randomized Study of the Pharmacokinetics of the Nutritional Supplement Nicotinamide Riboside (NR) and Its Effects on Blood NAD+ Levels in Healthy Volunteers. *PLoS ONE* **2017**, *12* (12), e0186459. https://doi.org/10.1371/journal.pone.0186459.

(23) Bernofsky, C.; Swan, M. An Improved Cycling Assay for Nicotinamide Adenine Dinucleotide. *Analytical Biochemistry* **1973**, *53* (2), 452–458. https://doi.org/10.1016/0003-2697(73)90094-8.
(24) Mayevsky, A.; Rogatsky, G. G. Mitochondrial Function in Vivo Evaluated by NADH Fluorescence: From Animal Models to Human Studies. *Am J Physiol Cell Physiol* **2007**, *292* (2), C615-640. https://doi.org/10.1152/ajpcell.00249.2006.
(25) Kawamitsu, H.; Hoshino, H.; Okada, H.; Miwa, M.; Momoi, H.; Sugimura, T. Monoclonal Antibodies to Poly(Adenosine Diphosphate Ribose) Recognize Different Structures. *Biochemistry* **1984**, *23* (16), 3771–3777. https://doi.org/10.1021/bi00311a032.
(26) Rudolph, J.; Roberts, G.; Muthurajan, U. M.; Luger, K. HPF1 and Nucleosomes Mediate a Dramatic Switch in Activity of PARP1 from Polymerase to Hydrolase. *eLife* **2021**, *10*, e65773. https://doi.org/10.7554/eLife.65773.
(27) Tong, L.; Lee, S.; Denu, J. M. Hydrolase Regulates NAD+ Metabolites and Modulates Cellular Redox. *Journal of Biological Chemistry* **2009**, *284* (17), 11256–11266. https://doi.org/10.1074/jbc.M809790200.
(28) Vives-Bauza, C.; Yang, L.; Manfredi, G. Assay of Mitochondrial ATP Synthesis in Animal Cells and Tissues. In *Methods in Cell Biology*; Elsevier, 2007; Vol. 80, pp 155–171. https://doi.org/10.1016/S0091-679X(06)80007-5.
(29) Menezes-Filho, S. L.; Amigo, I.; Prado, F. M.; Ferreira, N. C.; Koike, M. K.; Pinto, I. F. D.; Miyamoto, S.; Montero, E. F. S.; Medeiros, M. H. G.; Kowaltowski, A. J. Caloric Restriction Protects Livers from Ischemia/Reperfusion Damage by Preventing Ca2+-Induced Mitochondrial Permeability Transition. *Free Radical Biology and Medicine* **2017**, *110*, 219–227. https://doi.org/10.1016/j.freeradbiomed.2017.06.013.
(30) Fritsche-Guenther, R.; Bauer, A.; Gloaguen, Y.; Lorenz, M.; Kirwan, J. A. Modified Protocol of Harvesting, Extraction, and Normalization Approaches for Gas Chromatography Mass Spectrometry-Based Metabolomics Analysis of Adherent Cells Grown Under High Fetal Calf Serum Conditions. *Metabolites* **2019**, *10* (1), 2. https://doi.org/10.3390/metabo10010002.
(31) Abdel Rahman, A. M.; Pawling, J.; Ryczko, M.; Caudy, A. A.; Dennis, J. W. Targeted Metabolomics in Cultured Cells and Tissues by Mass Spectrometry: Method Development and Validation. *Analytica Chimica Acta* **2014**, *845*, 53–61. https://doi.org/10.1016/j.aca.2014.06.012.
(32) Milo, R.; Phillips, R. *Cell Biology by the Numbers*; Garland Science, Taylor & Francis Group: New York, NY, 2016.
(33) Hasmann, M.; Schemainda, I. FK866, a Highly Specific Noncompetitive Inhibitor of Nicotinamide Phosphoribosyltransferase, Represents a Novel Mechanism for Induction of Tumor Cell Apoptosis. *Cancer Research* **2003**, *63* (21), 7436–7442.

Figure legends

Figure 1: Chemical structure of the six adenine nucleotides analyzed here.

Figure 2: Schematic representation of the experimental workflow.

Figure 3: Separation profile of standards and linearity of standard curves. A: Chromatogram of standard analytes at 5 µg/mL concentration. ATP, ADP, ADPr, AMP and NAD^+ were run together, presented as "Mix" curve, and NADH was run separately. B: Standard curves for each analyte obtained in the conditions shown in A. Equations are represented as y = ax + b.

Figure 4: Simultaneous quantification of six adenine nucleotides in biological samples. A: representative chromatograms for each treatment, where NT: non-treated control; DMSO: 0.01% DMSO for 24h; FK866: 10 nM FK866 for 24h; FCCP: 20 µM FCCP for 2h; O2D: 1 µM oligomycin + 20 mM 2-deoxyglucose for 2h30min. B, C, D, E, F, G: concentration of each adenine nucleotide, normalized by protein mass in the extracts (µM/ µg of total protein). H, I, J: ratios of adenine nucleotides calculated from the data in B-G. Results are presented as mean ± standard deviation of 4 independent biological replicates, performed in duplicate.

Table 1: Limit of quantification (LOQ), linear regression parameters and estimation of loss due to the sample preparation procedure for each analyte.

	ATP	ADP	ADPr	AMP	NAD^+	NADH
LOQ (nM)	197	234	179	288	151	150
ax	41710.55	37471.07	44143.44	42515.46	51734.55	29716.56
b	15024.34	24459.71	23226.04	77089.39	31050.62	5308.98
R^2	0.99999	0.99997	0.99992	0.99973	0.99986	0.99999
Loss rate (%)	15.25	16.45	20.25	-18.70	15.29	30.27

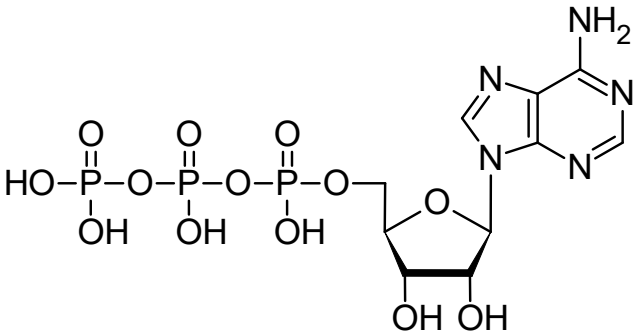

adenosine triphosphate
ATP

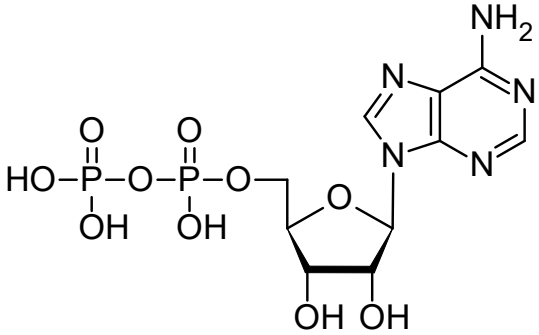

adenosine diphosphate
ADP

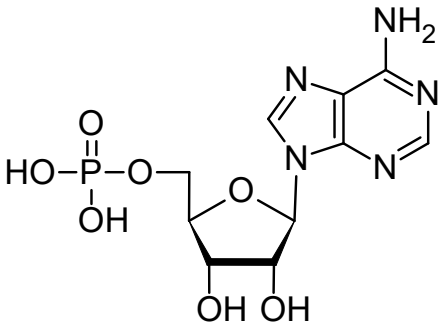

adenosine monophosphate
AMP

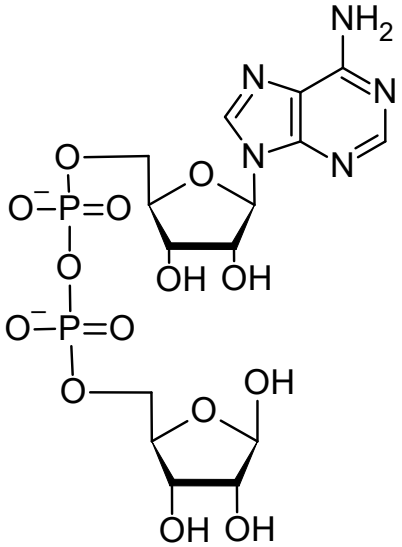

adenosine 5'-diphosphoriboside
ADPr

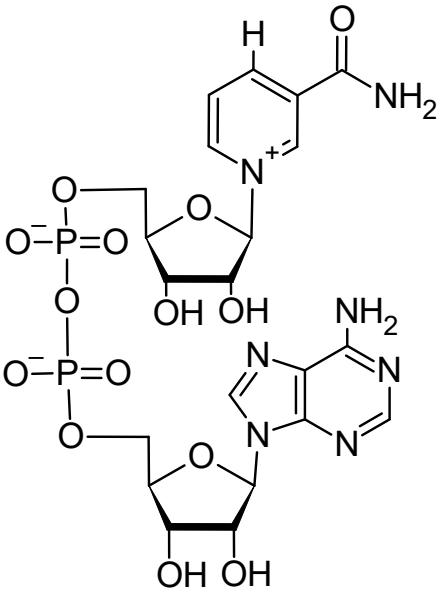

β-nicotinamide adenine dinucleotide
NAD⁺

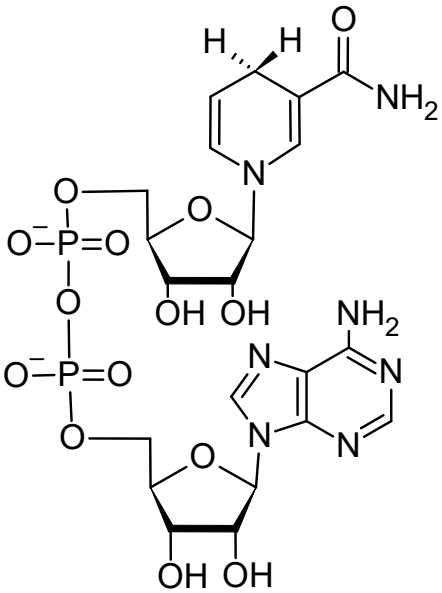

β-nicotinamide adenine dinucleotide reduced
NADH

Kopel et al., Figure 1

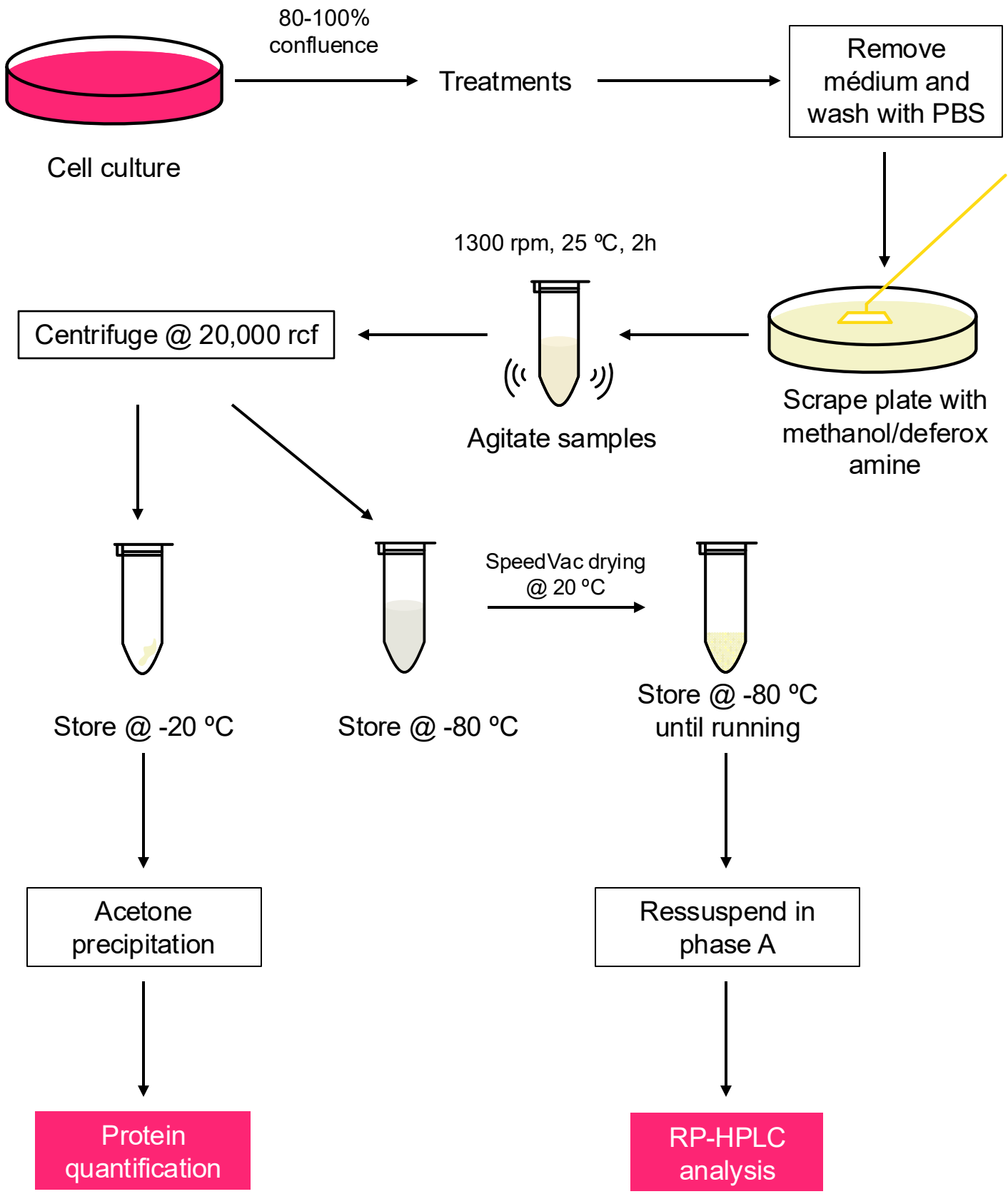

Kopel et al., Figure 2

A

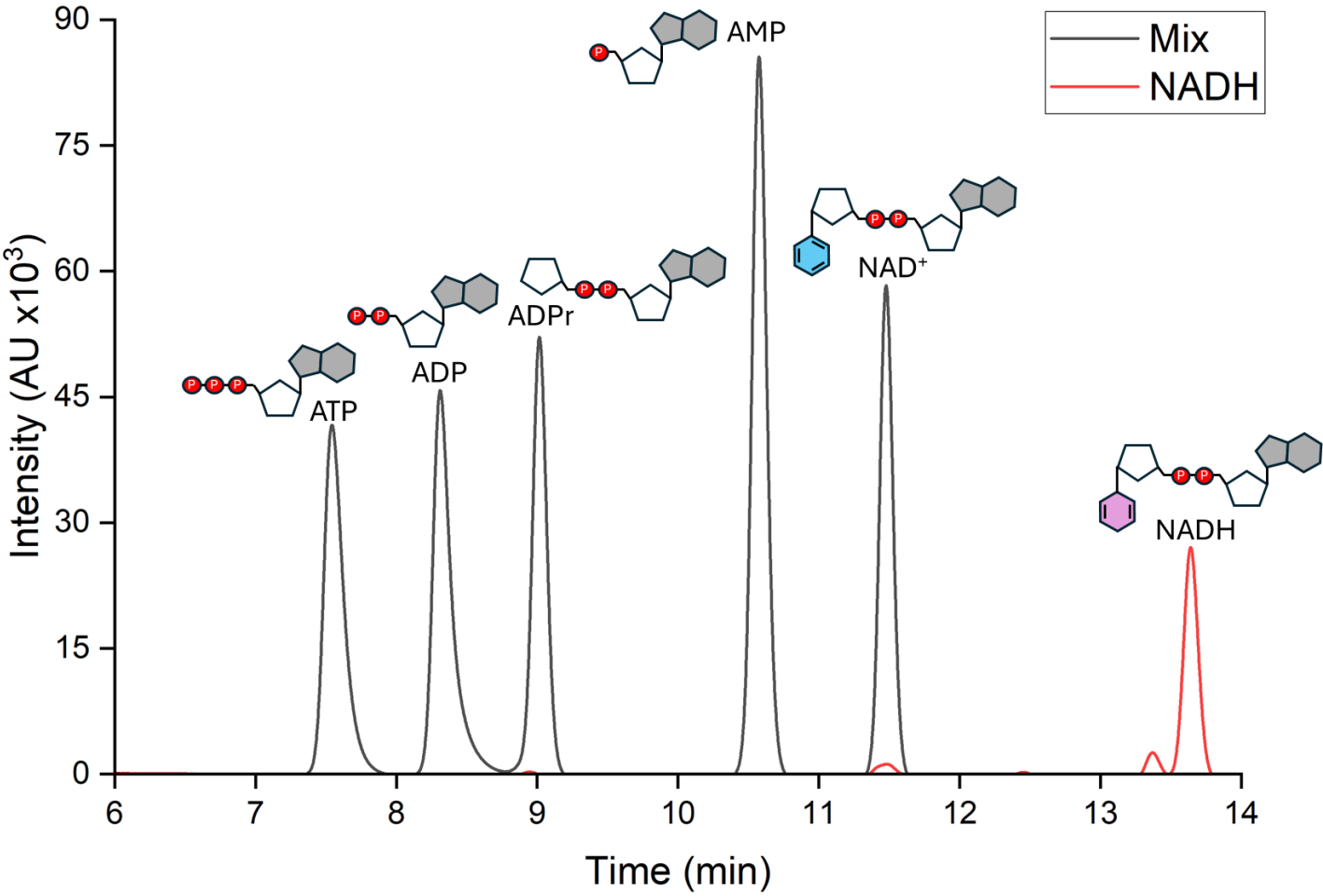

Kopel et al., Figure 3A

B

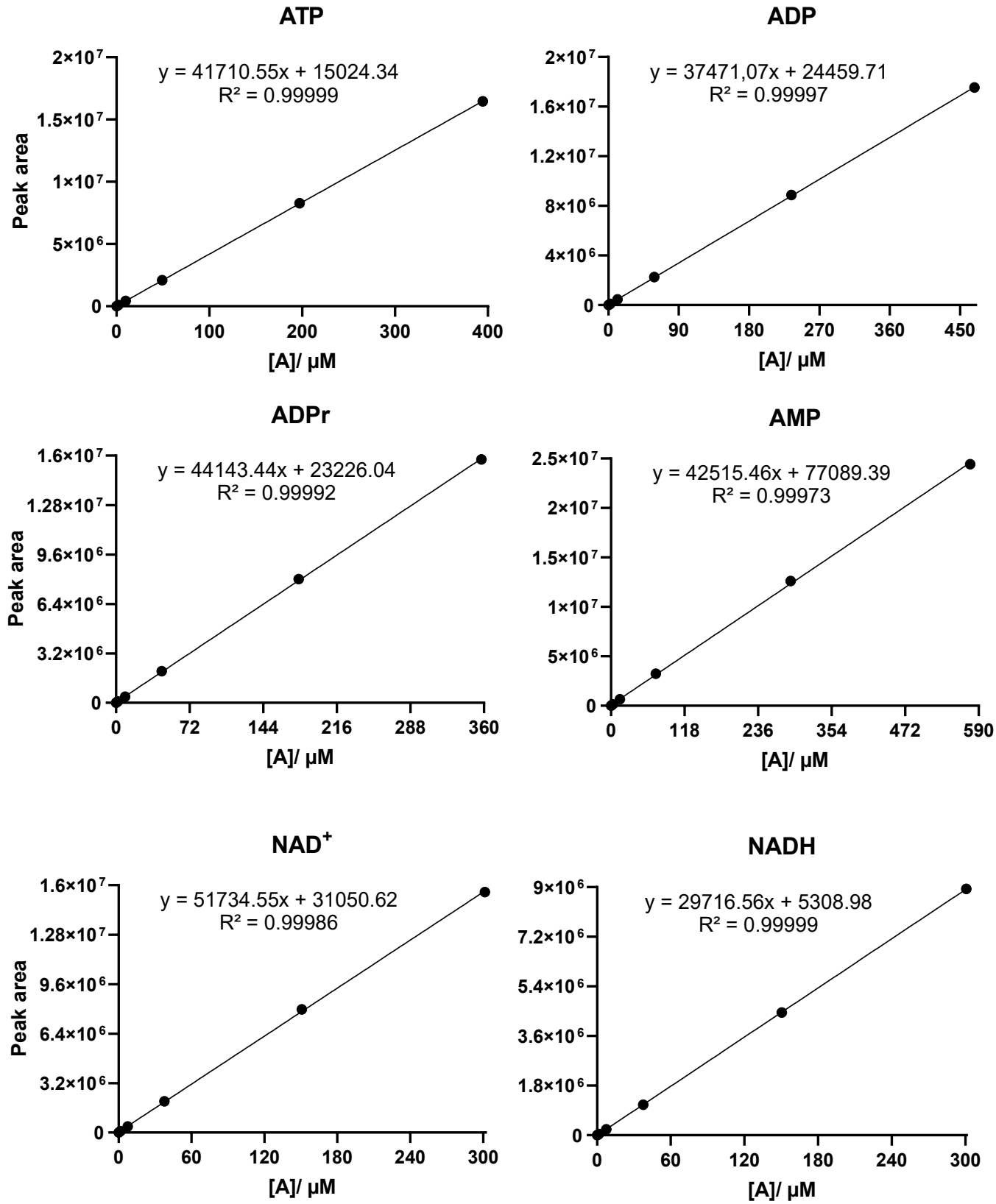

Kopel et al., Figure 3B

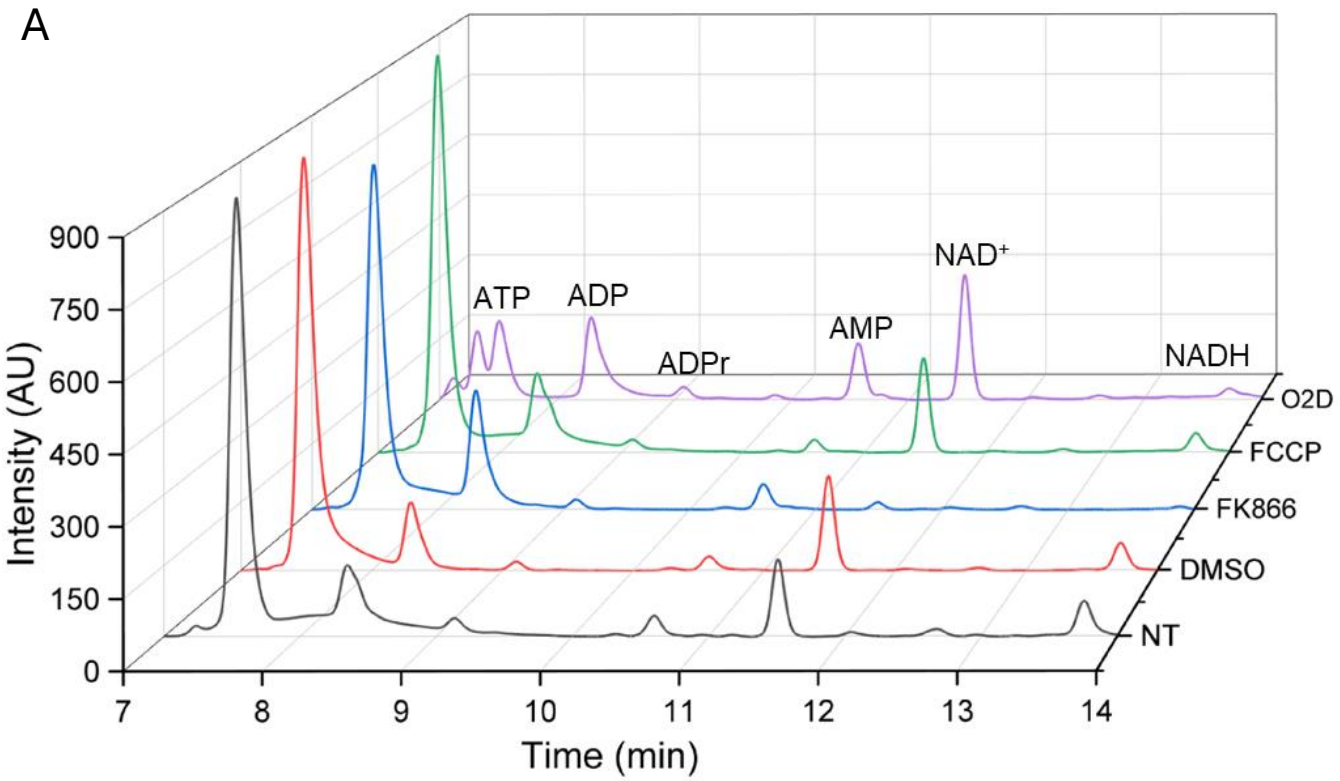

Kopel et al., Figure 4A

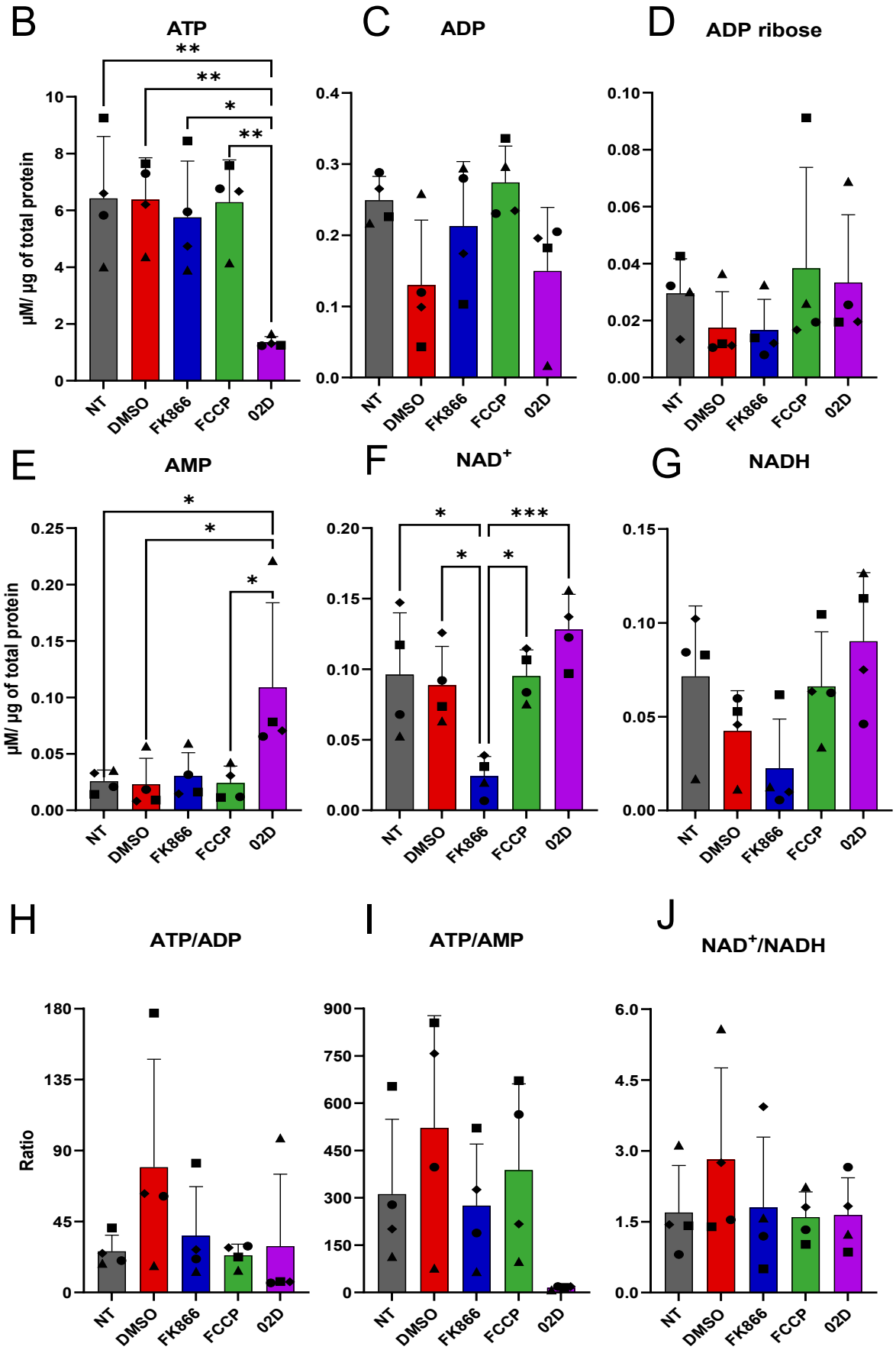

Kopel et al., Figure 4B-J